

Variable range hopping transport in ferromagnetic GaGdN epitaxial layers

A. Bedoya-Pinto, J. Malindretos, M. Roeber, D. D. Mai, and A. Rizzi

IV. Physikalisches Institut and Virtual Institute of Spin Electronics (VISE), Georg-August-Universität Göttingen, D-37077 Göttingen, Germany

(Received 4 June 2009; revised manuscript received 7 September 2009; published 17 November 2009)

Electrical-transport properties of ferromagnetic GaGdN layers grown by molecular-beam epitaxy on highly resistive 6H-SiC(0001) substrates have been investigated. It is found that doping with low concentrations of Gd increases the resistivity by several orders of magnitude as compared to unintentionally doped GaN. In the measurable temperature range between 5 and 120 K two different temperature dependences of the resistivity ($T^{-1/2}$ and $T^{-1/4}$) are observed, both of which are characteristic of variable-range-hopping conductivity in an impurity band of localized states. The experimental evidence, that room-temperature ferromagnetism and impurity-band hopping transport are coexistent, is discussed in connection with recent models proposing defect-induced magnetism in wide-band-gap III-Nitrides.

DOI: [10.1103/PhysRevB.80.195208](https://doi.org/10.1103/PhysRevB.80.195208)

PACS number(s): 71.55.Eq, 72.20.Ee, 72.25.-b, 61.72.uj

I. INTRODUCTION

Dilute magnetic semiconductors (DMSs) are intensively studied with the aim of achieving high spin polarization in material systems that can be suitably matched with present-day electronic devices. Although many groups have observed room-temperature ferromagnetism in a wide range of host semiconductors and magnetic dopants,¹ a major challenge is still a reproducible and well-defined preparation of DMSs layers and a comprehensive understanding of the magnetic coupling mechanisms. A promising host semiconductor for room-temperature ferromagnetism is GaN, for which doping with Gd has been reported to give a colossal room-temperature magnetic moment of around $1000\mu_B$ per magnetic impurity at low Gd concentrations.^{2,3} The authors attempted to explain the magnetic moment exceeding the $8\mu_B$ per Gd atom by an empirical model in which an extended polarization of the GaN matrix is assumed. However, x-ray magnetic circular dichroism experiments at the Ga *K* edge ruled out a significant polarization of the matrix.⁴ The generation of intrinsic defects in GaN layers by implantation of Gd³⁺ ions and the evolution of the saturation magnetization after annealing, point to the role of local magnetic moments on Ga and/or N interstitials.⁵ Other experimental reports attempt to explain that long-ranged ferromagnetic interactions in GaGdN are carrier induced, supported by the observed magnetization enhancement by Si codoping.⁶ Also the calculations by Dalpian and Wei⁷ support an electron stabilized ferromagnetism in GaGdN. Recent theoretical studies on the other hand come to the conclusion that Ga vacancies are crucial in inducing the ferromagnetic coupling in GaGdN.^{8,9} Moreover, the possibility that localized defect states without any magnetic ions may form local moments and exhibit collective magnetism has been investigated: cation vacancies in wide-band-gap nitrides might promote the formation of local magnetic moments, and the magnetic coupling between these defect-induced moments is supposed to be long ranged due to extended tails of the impurity wave function.¹⁰

In this work we present an experimental study of the electrical-transport properties of ferromagnetic GaGdN epitaxial layers, which might also help to clarify which picture

is suitable to interpret the still controversial origin of the room-temperature ferromagnetic coupling in GaGdN. It is shown that by Gd doping there is a transition from *n*-type-activated transport to variable-range hopping within an impurity band of localized states. The inferred hopping parameters suggest that Gd-induced defect states determine the electrical-transport behavior.

II. EXPERIMENT

GaGdN epitaxial layers have been grown by plasma-assisted molecular-beam epitaxy (MBE) with a Veeco UNI-Bulb nitrogen plasma source and effusion cells for the metal sources. The purity level of the source material is 7N for Ga and N and 4N for Gd. The growth was optimized on GaN/Al₂O₃ templates prepared by metalorganic vapor-phase epitaxy (MOVPE). The layers for electrical characterization were grown on semi-insulating 6H-SiC(0001) substrates, since the existence of more than one conductive channel or of a degenerate interface layer¹¹ does not allow a straightforward interpretation of the transport behavior. The epitaxy was carried out with the optimized parameters for the growth of undoped GaN, near the stoichiometric point in the slightly metal-rich regime at a substrate temperature of 760 °C.¹² For the Gd-doped samples the Gd cell was held at temperatures between 675 and 1400 °C. The layer thickness is about 500 nm.

The Gd concentration was measured by time-of-flight secondary ion mass spectroscopy (TOF SIMS). To increase the sensitivity of the measurement an oxygen background pressure of 10^{-6} mbar was applied. The detection limit is 10^{16} cm⁻³ for rare-earth elements and 10^{17} cm⁻³ for transition-metal elements as determined with ion-implanted Gd and Mn reference samples. The Gd concentration is mainly calculated from the ¹⁶⁰Gd peak because no mass interferences are expected there. To probe for transition-metal contaminations from the source, a sample with a high Gd concentration (10^{20} cm⁻³) was measured. Figure 1 shows an integrated mass spectrum. No transition-metal signals can be found in this sample, whereas the Gd isotopes are clearly visible. We conclude that the transition-metal contamination

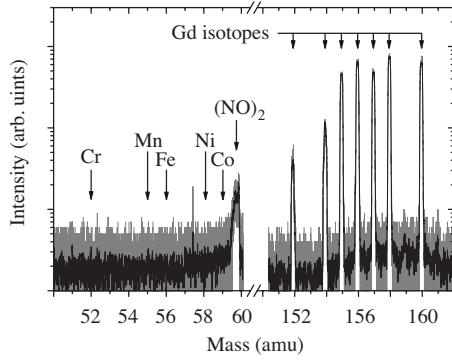


FIG. 1. Integrated TOF-SIMS spectrum of a 500-nm-thick GaGdN layer with a Gd concentration of 10^{20} cm^{-3} . The gray curve shows the raw data. Between 50 and 60 amu no traces of transition-metal elements are found. Between 152 and 160 amu the Gd isotopes are clearly revealed. The black curve shows a ten-point adjacent average smoothing of the raw data to reveal any hidden signals in the background.

is smaller than the Gd concentration by a factor of at least 10^{-3} .

Structural properties of the layers were investigated by means of a four-circle x-ray diffractometer (XRD). Magnetic characterization was performed with a superconducting quantum interference device in a temperature range of 2–300 K with a maximum field of 5 T. Electrical-transport measurements were performed using the van der Pauw geometry. Ohmic contacts were achieved by the deposition of a metallic Ti/Al/Ti/Au (30/160/40/50 nm) layer and subsequent rapid thermal annealing at 850 °C for 30 s. The temperature dependence of the resistivity has been measured between 5 and 300 K.

III. RESULTS

A. Structural and magnetic properties

Structural characterization by XRD shows that the samples grown on MOVPE-GaN and 6H-SiC(0001) have comparable crystalline quality; the full width at half maximum values of the rocking curves range from 400 to 524 arcsec for the (0002) Bragg reflection. In terms of secondary phases, only one sample in the upper concentration range (0.3 at. %) was found to contain GdN clusters in the cubic phase, with the crystallographic (111) direction parallel to the (0002) growth direction of the wurzite GaN. At concentrations below the detection limit of the XRD technique, x-ray linear dichroism measurements of the x-ray absorption near edge structures at the Gd L_3 and Ga K edges were performed on the same samples, which confirmed that Gd is substitutionally included in the GaN matrix.¹³

The magnetic properties show the same trend observed by Dhar *et al.*,^{2,3} where the average magnetic moment per Gd atom decreases with increasing concentration and finally saturates near its atomic moment. Except for the sample with GdN inclusions, which shows a ferromagnetic to paramagnetic transition at around 70 K, all samples are ferromagnetic at room temperature. This fact is a strong indication that the

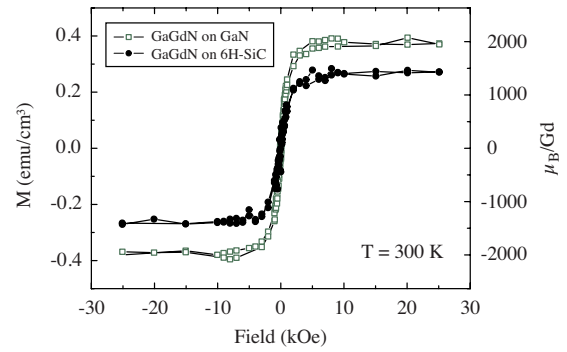


FIG. 2. (Color online) Room-temperature magnetization of two GaGdN layers with comparable Gd concentrations ($\sim 2 \times 10^{16}$ cm^{-3}) grown on different substrates. In agreement with Ref. 2 colossal magnetic moments are observed in both cases.

magnetic moment observed at room temperature cannot be originated by the GdN phase. Furthermore, the comparable room-temperature magnetization of GaGdN layers grown on two different substrates (Fig. 2) supports an effect related to the Gd incorporation rather than to substrate impurities. The coercivity is rather small, yielding values between 50 and 100 Oe.

B. Electrical transport

Even at moderate doping with Gd concentrations of 2×10^{16} cm^{-3} the resistivity shows an increase by nearly five orders of magnitude when cooling the sample from room temperature to 5 K (Fig. 3). A reference sample of pure GaN grown on semi-insulating SiC was measured for comparison. The unintentionally doped GaN grown by MBE is *n*-type with an activation energy of 21 meV and a background carrier concentration of 2×10^{17} cm^{-3} , known to be originated by shallow donors such as nitrogen vacancies or residual oxygen. Under the assumption that the native *n*-type doping is not significantly altered by the presence of Gd during growth, the highly resistive character of GaGdN suggests that Gd-induced deep states fully compensate these native donors.

The temperature dependence of the resistivity is depicted in Fig. 4. It does not follow the Arrhenius behavior, but scales with a power law $T^{-1/2}$ at lower temperatures

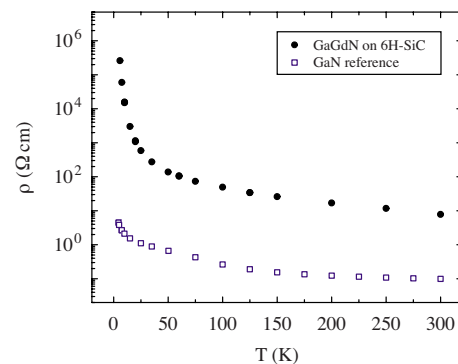


FIG. 3. (Color online) Temperature dependence of the resistivity of a GaN reference and a GaGdN epitaxial layer. The Gd concentration amounts to 2×10^{16} cm^{-3} .

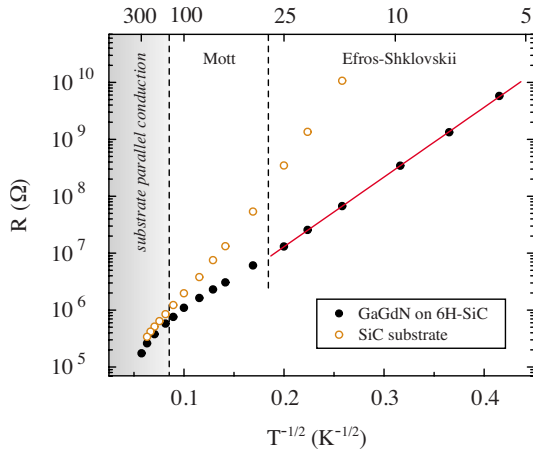


FIG. 4. (Color online) In the GaGdN sample, Efros-Shklovskii VRH behavior is found for temperatures below 25 K. In the intermediate temperature range the temperature dependence of the resistivity is characteristic of Mott VRH. Above 120 K, the conductivities of the GaGdN layer and the bulk substrate fall in the same order of magnitude.

($T < 25$ K) and with $T^{-1/4}$ in the intermediate temperature range. These power laws are characteristic of electronic transport by phonon-assisted hopping, e.g., by conduction in an impurity band of localized states with random spatial and energy distribution.¹⁴ Variable-range hopping (VRH) in three dimensions leads to a resistivity

$$\rho(T) = \rho_0 \exp[(T_0/T)^x], \quad (1)$$

where T_0 is the characteristic temperature and x is the hopping exponent. The exponent $x=1/4$ is derived when the density of states at E_F is assumed to be constant. This is known as the Mott-VRH regime.¹⁵ However, when many-electron interactions become important, the density of states will decrease quadratically with energy toward the middle of the impurity band, creating a soft gap in the DOS at the Fermi level, the so-called Coulomb gap. In this case, the exponent in Eq. (1) has been shown to be $x=1/2$, known as Efros-Shklovskii VRH (ES VRH).¹⁶

The degree of localization of the electronic states in the impurity band is described in terms of the localization length ξ which can be estimated from the characteristic temperature T_0 . In the ES-VRH regime, the localization length scales inversely proportional with $T_0^{(\text{ES})}$

$$\xi = \frac{\beta e^2}{k_B T_0^{(\text{ES})} \epsilon}, \quad (2)$$

where ϵ is the static dielectric constant and $\beta=2.8$ is a constant,¹⁷ e and k_B are the elementary charge and the Boltzmann constant, respectively. The static dielectric constant is composed of the normal host lattice and an additional contribution due to many-electron interactions, following the relation (in cgs units):^{17,18}

$$\epsilon = \epsilon_{\text{host}} + 4\pi e^2 N(E_F) \xi^2, \quad (3)$$

where $N(E_F)$ is the unperturbed DOS at the Fermi energy. In the Mott-VRH regime, $N(E_F)$ can be estimated from the

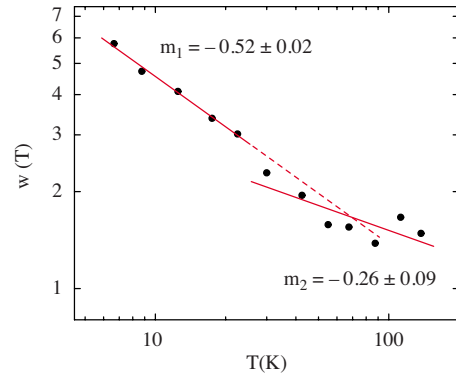


FIG. 5. (Color online) Transition from ES VRH to Mott VRH as determined by the method of Zabrodskii and Zinov'eva (Ref. 23).

Mott characteristic temperature $T_0^{(\text{Mott})}$ and the localization length ξ , as

$$N(E_F) = \frac{18}{k_B T_0^{(\text{Mott})} \xi^3}. \quad (4)$$

In order to calculate the hopping parameters without knowing $N(E_F)$, one has to be able to observe both the ES-VRH and the Mott-VRH regimes in the same sample. The transition occurs when, by increasing the temperature, the average carrier hopping energy ΔE_{hop} becomes larger than the coulomb gap Δ_{CG} , such that electron-electron interactions become comparably small, resulting in a smooth density of states at E_F . This transition has been measured in some other material systems such as indium oxide¹⁹ or boron-doped diamond.²⁰ Just few experimental studies of VRH transport in DMS layers are found in the literature.^{21,22} Concerning GaN-based DMS materials, Wu and Newman observed Mott VRH in Cr-doped GaN.²² Due to the lack of data from the ES-VRH regime, the value of $N(E_F)$ had to be taken from theoretical calculations in their analysis.

In our case, all the relevant parameters can be determined from experiment. The analysis of the temperature-dependent resistivity has been done according to the method of Zabrodskii and Zinov'eva,²³ which by starting from the general hopping law [Eq. (1)] provides a precise way to estimate the hopping exponents and thus distinguish between hopping regimes by plotting the quantity

$$w(T) = - \frac{\partial \ln \rho}{\partial \ln T} \cong - \bar{T} \frac{\Delta \ln \rho}{\Delta T} \quad (5)$$

against temperature on a log-log scale. ΔT is the temperature difference between two adjacent data points and \bar{T} denotes their average temperature. The result of the analysis of the GaGdN layer grown on SiC is shown in Fig. 5. The data in the ES-VRH regime (up to 25 K) can be well fitted, yielding a value of $x = -m_1 = (0.52 \pm 0.02)$ for the hopping exponent. In the Mott-VRH regime, the data are masked by the conductivity of the substrate for temperatures above 120 K. The temperature dependence of the resistivity in the intermediate temperature range can be fitted with an exponent of $x = -m_2 = (0.26 \pm 0.09)$. The characteristic temperature in the

different regimes is calculated based on Eq. (1) using the relation

$$T_0 = \left[-\frac{10^A}{m} \right]^{(-1/m)}, \quad (6)$$

where A is the intercept of the linear regression with the y axis and m denotes the slope of the fit. Using error propagation for the covariant variables A and m , one obtains values of $T_0^{(\text{ES})} = (657 \pm 186)$ K and $T_0^{(\text{Mott})} = (1.0 \pm 3.7) \times 10^5$ K for the characteristic temperatures. The large error, especially in the determination of $T_0^{(\text{Mott})}$ precludes a fully quantitative analysis of the hopping. Still, some important conclusions can be drawn from the evaluation of the hopping parameters.

These parameters, which are the localization length ξ , the static dielectric constant ϵ , and the unperturbed density of states at the Fermi level $N(E_F)$ in the impurity band, are fingerprints of the induced defects and can be determined from $T_0^{(\text{ES})}$ and $T_0^{(\text{Mott})}$ according to Eqs. (2)–(4). The obtained localization length is $\xi = (3.7 \pm 16)$ nm, and the static dielectric constant ϵ has a value of (19 ± 85) . This is an indication that GaGdN with $N_{\text{Gd}} = 2 \times 10^{16}$ cm $^{-3}$ is not in the critical regime close to the metal-insulator transition (MIT), where the anomalous contribution of ϵ becomes huge due to the divergence of the localization length. The critical behavior of ϵ when approaching the MIT is known as polarization catastrophe.²⁴ The obtained unperturbed density of states at the Fermi level amounts to $N(E_F) = (4.3 \pm 73) \times 10^{19}$ eV $^{-1}$ cm $^{-3}$. Another intrinsic property of the system is the coulomb gap energy Δ_{CG} , determined from the relation

$$\Delta_{CG} = \frac{e^3 N(E_F)^{1/2}}{\epsilon^{3/2}} \quad (7)$$

and yielding a value of (4.2 ± 8.0) meV. In order to evaluate the consistency of the derived hopping parameters, temperature-dependent quantities as the average hopping energy

$$\Delta E_{hop}^{(\text{ES})} = \frac{1}{2} k_B T (T_0^{(\text{ES})}/T)^{1/2} \quad (8)$$

or the average hopping distance

$$R_{hop}^{(\text{ES})} = \frac{1}{4} \xi (T_0^{(\text{ES})}/T)^{1/2} \quad (9)$$

have been calculated in the Efros-Shlikovskii regime, where the substrate contribution is negligible throughout the whole temperature range. At 25 K, the average hopping energy in the ES-VRH regime is $\Delta E_{hop}^{(\text{ES})} = (5.9 \pm 0.9)$ meV and lies close to the coulomb gap energy, an indication of the onset of the transition to the Mott-VRH regime. This is in agreement with the data presented in Fig. 5. Furthermore, for consistency the average hopping distance R_{hop} has to be larger than the localization length ξ and larger than the mean impurity distance. At the high-temperature boundary, where the smallest hopping distance is expected, we obtain $R_{hop}^{(\text{ES})}(25 \text{ K}) = (5.0 \pm 21)$ nm. Therefore, it is reasonable to assume that the first condition is fulfilled. However, assuming Gd as the impurity responsible for the VRH transport, the mean distance between two centers estimated from the experimental

Gd concentration would be $r_{\text{Gd-Gd}} = 41.6$ nm, which is larger than the inferred mean hopping distance, even considering the uncertainty in determining R_{hop} . In this case, the second condition would not be fulfilled. Moreover, at concentrations of $N_{\text{Gd}} = 2 \times 10^{16}$ cm $^{-3}$ it would not be possible to fully compensate the native donors in unintentionally doped GaN. Both arguments may suggest that other defects, which are present in a larger concentration than the Gd atoms, are the effective source for the electronic localization and VRH transport in GaGdN. These defects have to be acceptorlike, in order to compensate the shallow donors.

IV. DISCUSSION

Our electrical measurements clearly show the role of an acceptorlike defect in compensated ferromagnetic GaGdN. Gd itself can be ruled out as the responsible defect because the Gd concentration of 10^{16} cm $^{-3}$ is too low to fully compensate the background carrier concentration of 10^{17} cm $^{-3}$ and account for VRH transport in an impurity band. Furthermore, the observation of colossal magnetic moments cannot be explained by Gd solely, which suggests that the Gd-induced acceptors might also carry local magnetic moments.

The most commonly discussed defect with acceptor character in GaN is the Ga vacancy which is a triple acceptor. This defect has also been considered for its role in the ferromagnetism of GaGdN.^{8–10} Dev *et al.*¹⁰ investigated the formation of local magnetic moments for Ga vacancies in GaN without inclusion of any magnetic impurities by first-principles calculations. Neutral Ga vacancies are found to have an antiferromagnetic arrangement whereas charged states do couple ferromagnetically. This fits well with our observation of ferromagnetism in compensated GaGdN, since the partial filling of the impurity band will account for charged acceptor states. The authors also highlight that Ga vacancy states are localized but do possess extended defect wave-function tails. This fact is in qualitative agreement with our experimental observations of VRH transport with a localization length which turns out to be much larger than expected for $5d$ or strongly localized $4f$ -Gd states.

Another theoretical study by Gohda and Oshiyama⁹ investigates complexes of Gd impurities and Ga vacancies. It is found that the local moments of the Gd atoms and the Ga vacancies order ferromagnetically at room temperature. The authors suggest that the high magnetic moments observed in GaGdN arise mainly due to a high number of Ga vacancies per Gd atom. According to our experimental observations, magnetization values exceeding $1000\mu_B$ per Gd would require a ratio of $N_{\text{V}_{\text{Ga}}}/N_{\text{Gd}} \approx 300$ vacancies per Gd atom. For a Gd concentration of 2×10^{16} cm $^{-3}$ this would result in a Ga-vacancy concentration of about 6×10^{18} cm $^{-3}$, which would be high enough to fully compensate the native donors in our material. An experimental analysis of the defect distribution and an identification of the acceptorlike states would be the next step in order to verify if Ga vacancies are responsible for the observed VRH in ferromagnetic GaGdN.

The coexistence of ferromagnetism and variable-range hopping was studied by Sheu *et al.*²¹ for lightly doped GaMnAs. In this material system an impurity band of sub-

stitutional Mn acceptors is formed, and its compensation ratio can be changed by the controlled addition of As antisites which act as double donors. It has been shown that the mixed valences of the Mn acceptor will account for ferromagnetic behavior via a double-exchange mechanism.^{21,25} For the case of GaGdN, the situation is slightly different. A sizable concentration of acceptors is introduced even at very low Gd doping, forming an impurity band in which the electrons from the native donors are trapped. In both cases, the result is a partially filled impurity band where VRH transport occurs. Therefore, the scenario of double exchange between defect states with spatial and energetic disorder may be also applicable to GaGdN, given that the number and extension of defect states is enough to account for hybridization.

V. SUMMARY

In summary, we have performed a comprehensive study of the electrical-transport properties of ferromagnetic

GaGdN epitaxial layers grown by MBE. Doping with Gd, even at very low concentrations, results in a change from *n*-type band activated transport to variable-range hopping within an impurity band of localized states. In the measurable temperature range, the transition from Efros-Shklovskii to Mott VRH is observed. It is shown that other acceptor defects than Gd atoms are responsible for the compensation of the native donors and for the VRH transport behavior. It would be of great interest for the understanding of the observed colossal magnetic moments to identify the nature of these defects, and to quantify and correlate their number with the magnetic and transport properties in this material system.

ACKNOWLEDGMENTS

This work was partially supported by the Deutsche Forschungsgemeinschaft (Grant No. SFB 602) and the Virtual Institute of Spin Electronics (VISel). We thank U. Zastrow (Forschungszentrum Jülich) and P. J. Wilbrandt (Universität Göttingen) for performing the SIMS measurements.

-
- ¹T. Dietl, *J. Phys.: Condens. Matter* **19**, 165204 (2007).
²S. Dhar, O. Brandt, M. Ramsteiner, V. F. Sapega, and K. H. Ploog, *Phys. Rev. Lett.* **94**, 037205 (2005).
³S. Dhar, L. Perez, O. Brandt, A. Trampert, K. H. Ploog, J. Keller, and B. Beschoten, *Phys. Rev. B* **72**, 245203 (2005).
⁴A. Ney, T. Kammermeier, V. Ney, S. Ye, K. Ollefs, E. Manuel, S. Dhar, K. H. Ploog, E. Arenholz, F. Wilhelm, and A. Rogalev, *Phys. Rev. B* **77**, 233308 (2008).
⁵M. A. Khaderbad, S. Dhar, L. Perez, K. H. Ploog, A. Melnikov, and A. D. Wieck, *Appl. Phys. Lett.* **91**, 072514 (2007).
⁶Y. K. Zhou, S. W. Choi, S. Emura, S. Hasegawa, and H. Asahi, *Appl. Phys. Lett.* **92**, 062505 (2008).
⁷G. M. Dalpian and S.-H. Wei, *Phys. Rev. B* **72**, 115201 (2005).
⁸L. Liu, P. Y. Yu, Z. Ma, and S. S. Mao, *Phys. Rev. Lett.* **100**, 127203 (2008).
⁹Y. Gohda and A. Oshiyama, *Phys. Rev. B* **78**, 161201(R) (2008).
¹⁰P. Dev, Y. Xue, and P. Zhang, *Phys. Rev. Lett.* **100**, 117204 (2008).
¹¹D. C. Look and R. J. Molnar, *Appl. Phys. Lett.* **70**, 3377 (1997).
¹²The substrate temperature is to be understood as an internal reference due to the known problems in measuring the surface temperature of transparent substrates by pyrometry.
¹³G. Martinez-Criado, O. Sancho-Juan, N. Garro, J. Sans, A. Cantarero, J. Susini, M. Roever, D.-D. Mai, A. Bedoya-Pinto, J. Malindretos, and A. Rizzi, *Appl. Phys. Lett.* **93**, 021916 (2008).
¹⁴M. Pollak, *Phys. Status Solidi B* **230**, 295 (2002).
¹⁵N. F. Mott, *Philos. Mag.* **19**, 835 (1969).
¹⁶A. L. Efros and B. I. Shklovskii, *J. Phys. C* **8**, L49 (1975).
¹⁷A. L. Efros and B. I. Shklovskii, in *Electronic Properties of Doped Semiconductors*, edited by M. Cardona (Springer, New York, 1984), p. 235.
¹⁸T. G. Castner, in *Hopping Transport in Solids*, edited by M. Pollak and B. Shklovskii (North-Holland, Amsterdam, 1991), p. 10.
¹⁹R. Rosenbaum, *Phys. Rev. B* **44**, 3599 (1991).
²⁰T. Sato, K. Ohashi, H. Sugai, T. Sumi, K. Haruna, H. Maeta, N. Matsumoto, and H. Otsuka, *Phys. Rev. B* **61**, 12970 (2000).
²¹B. L. Sheu, R. C. Myers, J.-M. Tang, N. Samarth, D. D. Awschalom, P. Schiffer, and M. E. Flatte, *Phys. Rev. Lett.* **99**, 227205 (2007).
²²S. Y. Wu and N. Newman, *Appl. Phys. Lett.* **89**, 142105 (2006).
²³A. G. Zabrodskii and K. N. Zinov'eva, *Zh. Eksp. Teor. Fiz.* **86**, 727 (1984) [*Sov. Phys. JETP* **59**, 425 (1984)]; A. G. Zabrodskii and A. G. Andreev, [*JETP* **58**, 756 (1993)].
²⁴T. G. Castner, N. K. Lee, G. S. Cieloszyk, and G. L. Salinger, *Phys. Rev. Lett.* **34**, 1627 (1975).
²⁵S. C. Erwin and A. G. Petukhov, *Phys. Rev. Lett.* **89**, 227201 (2002).